Science of the Total Environment 785 (2021) 147321

Contents lists available at ScienceDirect

Science of the Total Environment

journal homepage: www.elsevier.com/locate/scitotenv

Glacier changes on the Nanga Parbat 1856–2020: A multi-source retrospective analysis

Marcus Nüsser [a,b,*], Susanne Schmidt [a]

[a] Department of Geography, South Asia Institute, Heidelberg University, Heidelberg 69115, Germany
[b] Heidelberg Centre for the Environment, Heidelberg University, Heidelberg 69120, Germany

HIGHLIGHTS

- Analysis of Himalayan glacier changes over a very long observation period (1856–2020).
- Integration of multi-source historical and remote sensing data sets
- Avalanches have a major impact on glacier dynamics of the mountain massif.
- Individual glaciers show surge-type ice movement due to high relief energy.
- Nanga Parbat glacier dynamics show similarity to the Karakoram Anomaly.

GRAPHICAL ABSTRACT

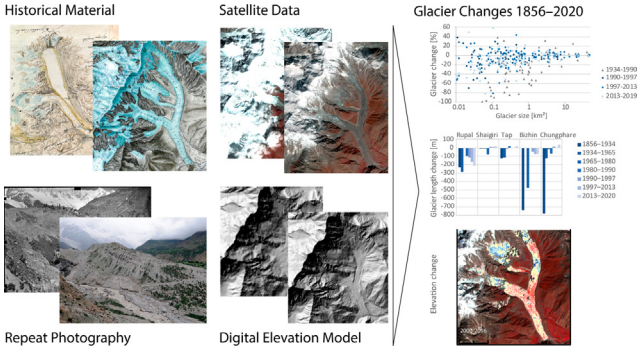

ARTICLE INFO

Article history:
Received 22 February 2021
Received in revised form 17 April 2021
Accepted 19 April 2021
Available online 24 April 2021

Editor: A P Dimri

Keywords:
Cryosphere change
Multi-source analysis
Repeat photography
Upper Indus Basin
Himalaya
Nanga Parbat

ABSTRACT

Contemporary changes in the Himalayan cryosphere are an important concern in the global climate change debate. In this context, the glaciers of the Upper Indus Basin (UIB) deserve special attention because of their importance for freshwater supply in the mountain valleys and the adjoining lowlands. However, detailed long-term glacier monitoring studies are rare due to the lack of historical data with adequate spatial and temporal resolution. In the case of Nanga Parbat, the ample availability of historical maps and terrestrial photographs together with satellite imagery and digital elevation models make it possible to analyse and quantify glacier changes for the period between 1856 and 2020. Using diverse multi-temporal datasets, this study reveals slight changes in ice-covered area for 63 glaciers, which decreased by 7% between 1934 and 2019. A detailed analysis of five glaciers in the Rupal Valley over the period 1856–2020 identifies diverse response patterns and highlights the importance of ice and snow avalanches, surge-type instabilities and site-specific topographic particularities for individual glacier changes. The results show high similarity with the stable glacier mass in the Karakoram. This study demonstrates the advantages of combining multiple sources and types of data in order to achieve consilience and offer robust insights.

1. Introduction

The consequences of detected and expected changes in the South Asian cryosphere have become a global concern in the aftermath of the IPCC glacier controversy 2007 (Bolch et al., 2012; Cogley, 2011; Hock et al., 2019; Nie et al., 2021). Due to their hydrological importance, the glaciers in the Upper Indus Basin (UIB) have aroused considerable research interest and media coverage (Immerzeel et al., 2020; Nüsser and Baghel, 2014). Many studies are solely or predominantly based on multi-temporal analyses of remote sensing data usually without adequate ground truthing. However, long-term glacier studies in the wider Himalayan region that extend the observation period to the

* Corresponding author at: Department of Geography, South Asia Institute, Heidelberg University, Heidelberg 69115, Germany.
E-mail address: marcus.nuesser@uni-heidelberg.de (M. Nüsser).

https://doi.org/10.1016/j.scitotenv.2021.147321

time before ubiquitous availability of satellite data are limited to a few exceptions (Chand et al., 2017; Rashid and Majeed, 2020; Shukla et al., 2017). This can essentially be traced back to the scarcity of ground-based measurements and related historical datasets with adequate spatial and temporal resolution (Bhambri and Bolch, 2009). Given the availability of suitable historical glacier images, the integration of terrestrial repeat photography can provide the necessary information, as demonstrated in different mountain regions (Byers, 2007, 2000; Kamp et al., 2013; Nüsser, 2001).

While a large number of studies in the UIB focus on changes in glacier lengths, glacier-covered areas and ice volumes, the Nanga Parbat massif has received little attention in remote sensing studies combined with ground surveys over the last two decades (Muhammad et al., 2019a). The ongoing discussion on the Karakoram anomaly (Farinotti et al., 2020; Hewitt, 2005; Kääb et al., 2012; Muhammad et al., 2020), which characterises the hydro-climatic peculiarities of the great divide between the drainages of Central Asia and the UIB, has initiated a recent increase in research on glacier surges (Bhambri et al., 2017; Copland et al., 2011; Gardelle et al., 2012; Hewitt, 2007; Paul, 2019, 2015). Being part of the north-western Himalaya, Nanga Parbat is located less than 75 km to the south of the Karakoram range, from which it is separated by the Indus river. Thus, certain climatic and glaciological similarities between these two adjacent high mountain regions can be assumed. Besides the specific location and transitional hydro-climatic position of the Nanga Parbat massif, the local study of glacier changes in this western part of the UIB is justified by the availability of rare long-term glaciological data on this mountain starting with the observations by Adolph Schlagintweit in 1856 (Kick, 1967). The long monitoring period is based on multi-source archival material, such as historical sketch maps and topographical maps, and a comprehensive collection of landscape photographs, taken by members of various historical expeditions (Finsterwalder, 1938; Kick, 1994). This material offers a rare long-term perspective not just for the analysis of glacier changes, but also glacier and meltwater related livelihood strategies and local development trajectories (Nüsser, 2000; Nüsser and Schmidt, 2017). The present study aims to analyse and quantify glacier changes on the Nanga Parbat between 1856 and 2020. It is based on the hypothesis that the combination of multi-source archival material with remote sensing imagery provides more detailed information on glacier changes over a long monitoring period.

2. Study area

The massif of Nanga Parbat (8126 m a.s.l.; 35°14′N, 74°35′E) constitutes the north-western anchor of the greater Himalayan range. Located in Gilgit-Baltistan, Pakistan, the prominent mountain towers more than 7000 m above the gorge of the Indus river and more than 4500 m over the Rupal Valley (Fig. 1). This distinct topographic prominence and isolation together with the enormous relief energy affects hydro-climatic conditions and glacier distribution. The transitional position of Nanga Parbat between monsoonal influences in summer and winter precipitation dominated by western disturbances is overlaid by steep altitudinal temperature and precipitation gradients, which range from arid valley floors to the higher ridges with regular snowfall throughout the year (Dahri et al., 2016; Farhan et al., 2015; Winiger et al., 2005).

The debris-covered valley glaciers are largely sustained by avalanches, which cause a significant re-distribution of ice and snow from the accumulation to the ablation zones over long vertical distances (Fig. S1). According to the typology discussed by von Wissmann (1959) and Hewitt (2011), these glaciers either belong to the "Turkestan" or the "Mustagh" type, both characterised by the huge importance of snow and ice avalanches. Whereas the "Turkestan" type ice streams have no accumulation zones and are almost entirely avalanche-fed, the "Mustagh" type ice streams start in the accumulation zone but are also predominantly fed by avalanches. Within the large valley glaciers, the Rupal Glacier is the only one which is mainly fed by snow fall and belongs to the "Alpine" type. Additionally, small clean ice glaciers located in cirques and hanging glaciers in niches can be found.

The massif of Nanga Parbat is characterised by a long history of glaciological research. The earliest studies were carried out around the end of the Little Ice Age, when Adolph Schlagintweit visited the Rupal Valley in 1856. Besides landscape paintings, sketch maps and descriptions, he differentiated between debris-covered and clean ice glaciers. Other scientific reports were given by colonial administrative officers and travellers, who presented reports on glacier lake dynamics and surface changes of glaciers in the Rupal Valley (Collie, 1897; Drew, 1875; Neve, 1907). Extensive and systematic field surveys of the entire mountain massif were initiated by the German Himalaya Expedition in 1934, resulting in topographical maps of Nanga Parbat at scales of 1:50,000 and 1:100,000 using terrestrial photogrammetry (Finsterwalder, 1938). A special focus of this expedition was on glacier distribution, dynamics and velocities (Finsterwalder, 1937). Glaciological research activities in the region continued in 1937 (Troll, 1938), 1958 (Kick, 1967; Loewe, 1961) and 1987 (Kick, 1994; Kuhle, 1996). More recent studies from the massif mostly concentrate on individual glaciers or tributary basins (Gardner, 1986; Muhammad and Tian, 2016; Muhammad et al., 2019a; Schmidt and Nüsser, 2009; Shroder et al., 2000).

3. Data and methods

A multi-temporal and multi-source approach, based on remote sensing data, repeat terrestrial photography and related historical information was used to detect and analyse glacier changes on the Nanga Parbat over the past 164 years (1856–2020). While Landsat data are useful for the monitoring of glacier dynamics and variations since the 1970s, Corona and Hexagon images from the early US military reconnaissance missions extended the time span for detecting changes back to the 1960s. The toposheets and photographs from 1934 enabled a quantification of glacier changes over the past 86 years and the sketch map and paintings by Schlagintweit extended glacier length analysis for the Rupal Valley to the mid of the 19th century. Relevant historical material was collected from archives and collated for multi-temporal analyses.

3.1. Historical data

The 1934 topographic map at a scale of 1:50,000 (Finsterwalder, 1938) is remarkable for its highly accurate contour lines (contour interval: 50 m), river outlines and glacier margins. As the uppermost part of the Rupal Valley and parts of the Diamir Valley are not shown on this map, the additional 1:100,000 map (contour interval: 100 m) surveyed by the same expedition was used. However, the Diamir Glacier and the other glaciers to the south of Rupal Valley were excluded from change detection analyses as the mapping accuracy of these areas is somewhat uncertain due to the lack of photogrammetric surveys in 1934. The scanned and georeferenced 1934 toposheet (projected on the Everest ellipsoid, Gauss-Krüger system) was used to investigate changes in glacier area and length. A scan of an unfolded copy of this map (600 dpi) was co-registered to the Landsat image from 2019 using 22 ground control points with a root mean square (RMS) error of 11, using a pixel size of 2.5 m, thereby reaching subpixel accuracy on Landsat imagery. Visual comparison of the co-registered map and satellite images confirmed the requisite high spatial accuracy.

As the 1856 sketch map of the glaciers of the Rupal Valley produced by Schlagintweit (Fig. S2) shows only the ice streams, rivers and main relief structures without an exact scale (Kick, 1967; Nüsser, 2015), co-registration was not feasible. However, visual comparison of this sketch map with a high spatial resolution QuickBird image enabled reconstruction of the former positions of some glaciers. Additional information such as the extent of debris-cover and particular surface structures like ogives on the Chungphare Glacier were derived from visual

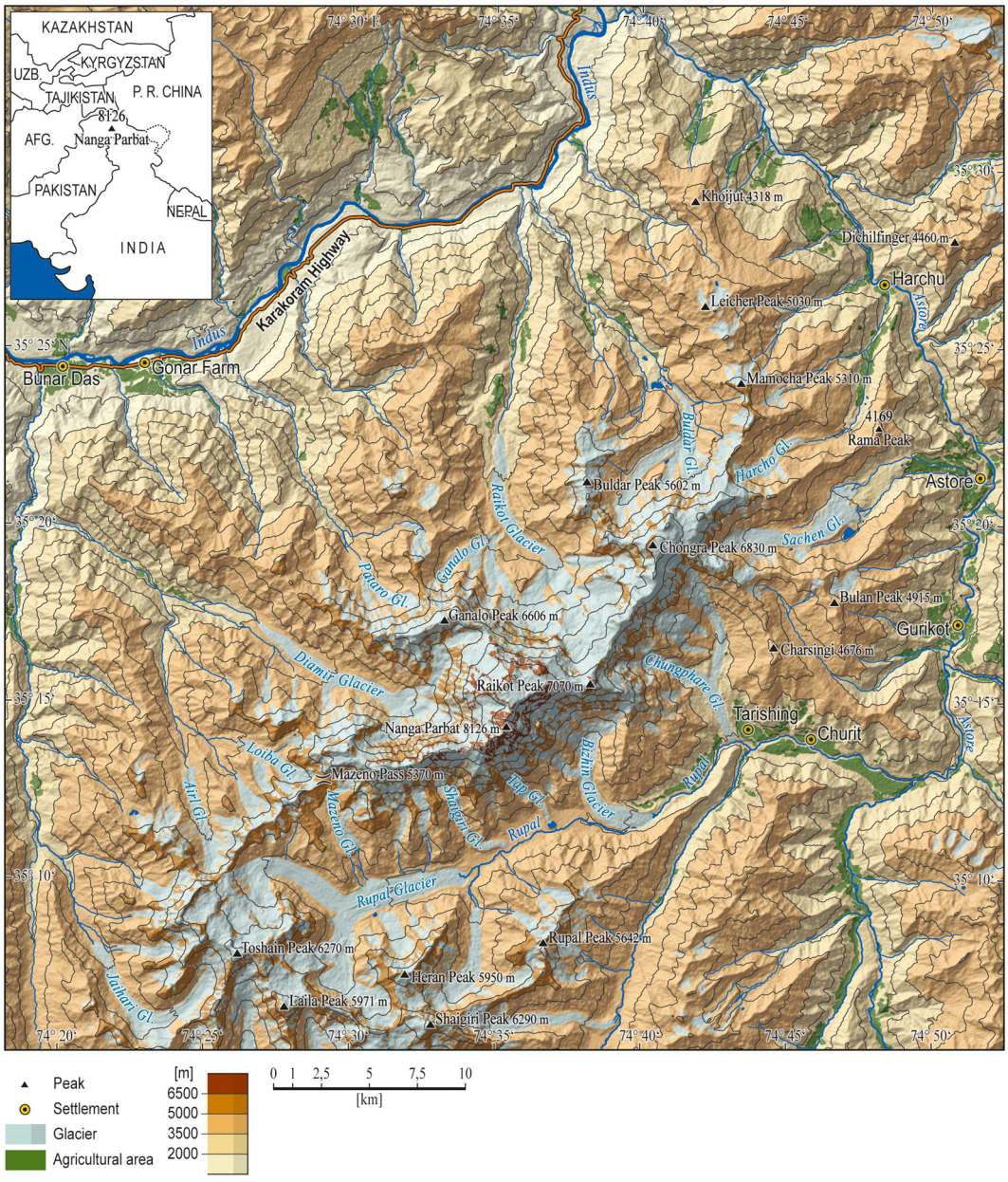

Fig. 1. The mountain massif of Nanga Parbat in the north-western Himalaya.

interpretation of the sketch map. Archival material from the Schlagintweit collections was obtained from the Bavarian State Library (Archive Schlagintweitiana) and the German Alpine Club.

3.2. Repeat photography

The study also combined historical glacier photographs taken during various expeditions to Nanga Parbat with matched photographs. A comprehensive collection of historical photographs and additional visual material (see Table 1, Data in Brief) enabled multi-temporal comparisons and monitoring. The metric photographs acquired during surveys in 1934, 1958 and 1987, originally taken on glass plates (13 cm × 18 cm) and stored at Technical University Munich, were scanned at high resolution (600 dpi) as a baseline dataset. Several re-photographic surveys carried out between 1992 and 2010 allowed for comparisons and visual evidence of glacier changes. Particular emphasis was laid on glacier fluctuations, changes in ice volume and in the ratio between debris-covered and clean ice glacier parts. For this purpose, it was possible to repeat a large number of historical photographs from viewpoints identical to the earlier ones (Dickoré and Nüsser, 2000; Nüsser, 2000; Schmidt and Nüsser, 2009).

3.3. Satellite imagery and digital elevation models

Landsat images from the years 1990, 1997, 2010, 2013, 2019 and one Sentinel-2 image from 2020 (Table S1) were used to delineate glacier boundaries using a standardized semi-automatic approach based on red/shortwave Infrared band ratio (Paul et al., 2016). All Landsat images are from the Collection 1 Tier 1, which show a low georegistration RMS error of <12 m and are suitable for change detection analysis (Dwyer et al., 2018). In order to reduce the impact of sensor degradation or varying radiometric resolution, Landsat images were radiometrically calibrated to top-of-atmosphere reflectance (Young et al., 2017). A threshold of 2.4 was set for all ratio bands derived from Landsat images

and a higher threshold of 3.2 was set for the ratio band derived from Sentinel-2 image in order to delineate clean ice and perennial snow.

Although the band ratio method is robust and time-efficient in delineating clean ice, additional manual correction of debris-covered glacier boundaries was necessary (Racoviteanu et al., 2009). In order to reduce the impact of seasonal snow, only satellite images from the end of the ablation period were selected. Furthermore, snow covered pixels which appeared as snow-free in 1997 were manually removed in the images from 2013 and 2020. This correction was supported by visual comparison with Planet data from 2020. The classified ice and snow covered areas were separated into entities on the basis of watersheds extracted from the Global Advanced Spaceborne Thermal Emission and Reflection Radiometer Digital Elevation Model (GDEM) by using the Hydrology Tool in ArcGIS 10.6, and then manually corrected. For further analysis, the separated ice and snow covered areas were transformed to vector data and all polygons smaller than 0.01 km^2 were deleted (Paul et al., 2010; Schmidt and Nüsser, 2012). Debris-covered glacier tongues were digitized manually (Racoviteanu et al., 2009), as DEMs were not available for all observation periods (Paul et al., 2004). For the glacier inventory, topographic parameters (elevation, aspect, slope) were derived by using the void-filled Shuttle Radar Topography Mission (SRTM)-DEM with a spatial resolution of 30 m. Due to monsoonal influences, most summer images of the study area are cloud- or snow-covered. Thus, the number of images suitable for the current study was reduced considerably. As the Corona image from 1965 is heavily snow-covered and the Hexagon image from 1980 is partly cloud-covered, overexposure hampered the differentiation between snow- and ice-covered and snow-free areas. Therefore, digitized glacier tongues on the co-registered images were used solely for glacier length analysis. For maximum glacier length, central flowlines were drawn based on the SRTM-DEM and the terminus variations were measured between the cut segments (Schmidt and Nüsser, 2017).

Multi-temporal glacier analysis with various satellite datasets reveals uncertainties due to the pixel size and co-registration of satellite data. The uncertainty was estimated with a buffer of half a pixel size for each glacier, as recommended by Granshaw and Fountain (2006) and applied in several studies (Bhambri et al., 2011; Bolch et al., 2010). Thus, the uncertainty was ±15 m for Landsat and ±5 m for Sentinel imagery, respectively. The error estimation was calculated by the standard deviation of the sum of the error for each glacier (Gardent et al., 2014).

Avalanche deposits on the Bizhin glacier were mapped to identify their extent and frequency. For this purpose, satellite images with high to very high spatial resolution are required in order to differentiate between fresh snow and avalanche deposits with rough surface structures. Despite the development of several automatic classification approaches (Eckerstorfer et al., 2016; Lato et al., 2012), avalanche deposits were mapped manually in summer images when most seasonal snow cover has melted in the runout zones. Planet data were used for the period 2017–2020. One KOMPSat-2 (Korea Multi-Purpose Satellite) image from 2008 and one QuickBird image from 2003 were added in order to increase the number of measurements.

In order to quantify elevation changes of glacier surfaces in the Rupal Valley, the differences of three DEMs generated from the 1934 toposheet, the SRTM and the High Mountain Asia (HMA) 8-meter DEM were calculated (Table 3). The SRTM-DEM v3 (February 11–22, 2000) with a spatial resolution of 30 m formed the basis for this measurement. However, along the Himalayan arc, the DEM contains large amounts of data voids which were filled with interpolated data thereby reducing the accuracy of the SRTM heights (Mukul et al., 2017). In order to exclude these interpolated parts from the analysis, the filled voids were masked. The HMA 8-meter DEM is generated from very-high-resolution satellite imagery launched by Digital Globe in order to support studies on glacier changes in the Tien Shan, Hindu Kush and Himalaya. The data are distributed by the NASA National Snow and Ice data Center (Shean, 2017). Overall, the data are characterised by a high quality; however, many data voids exist and the DEMs are often of a small coverage. As no DEM covering the entire Nanga Parbat massif or the entire Rupal Valley was available, three HMA-DEMs from 2013, 2014 and 2016 were used to analyse surface changes since 2000. Due to the steepness of the Nanga Parbat south face, most DEMs show data voids at higher altitudes. Some studies in the Himalaya and Karakoram faced the same problems in DEM-based glacier volume change estimations (Gardelle et al., 2013; Maurer et al., 2016). Following the approach by Maurer et al. (2016), slopes steeper than 30° were not considered for surface changes in the present study. Consequently, the elevation change analysis was restricted to the ablation zone where most glaciers are debris-covered, which in turn reduced the impact of the uncertain C-band penetration in snow and ice, which varies between 2.4 m (Gardelle et al., 2012) and 6 m (Kääb et al., 2015).

Based on digitized contour lines with an equidistance of 50 m, together with altitudinal points, and streams shown in the 1934 topographical map (Spohner, 2004), a DEM was generated using the Topo to Raster tool in ArcGIS 10.6. The DEM with a spatial resolution of 30 m was co-registered to the SRTM-DEM using an interest operator in ENVI 5.6. Points with a high RMS error and points located on unstable terrain on and around glaciers were deleted. The DEM 1934 was co-registered with well-distributed 66 points and a RMS-error smaller than 1. In order to reduce the planimetric and vertical shift (mean difference), all DEMs were adjusted to the SRTM. The vertical adjustment factors were calculated on ice-free and stable ground (slope angles less than 30°) excluding the interpolated void-filled areas of the SRTM-DEM and the standard error between the corrected altitudes are presented in Table S2.

For an overview, all data, methods and approaches used in this study are summarized in a workflow (Fig. 2).

4. Results

4.1. Glacier inventory

A total of 92 glaciers and perennial snow fields larger than 0.01 km^2 covered an area of about 299.6 ± 24.1 km^2 in 2019. Kick (1994) only reported 69 glaciers in the Nanga Parbat region based on the 1934 toposheet. This difference is caused by the inclusion of the entire Diamer Valley, small glaciers and perennial ice fields in the inventory presented here, which are not shown in the map from 1934. About one third of all glaciers (31) and glacier covered area (130.4 ± 10.6 km^2) are located in the Rupal Valley. 65 glaciers (71%) of the entire study area are smaller than 1 km^2, which cover a total area of about 14 km^2, and seven glaciers are larger than 10 km^2 with a total area of 207.2 ± 13.0 km^2 (69%). The three largest glaciers Rupal (46.1 ± 2.1 km^2, length: 16.6 km) in the south, Diamir (42.7 ± 3.1 km^2, length: 14.3 km) in the west and Raikot (42.3 ± 1.7 km^2, length: 15.9 km) in the north of the massif cover 43% of the glacier-covered area. Whereas clean ice glaciers and perennial snow patches are dominant in the size class of less than 1 km^2, almost all larger glaciers are debris-covered (Fig. 3A). In total, around one third of all glaciers (27 glaciers) are debris-covered (282.8 ± 20.9 km^2), where the total debris-coverage of glaciers in the Nanga Parbat area measures 67.9 km^2 which amounts to 22.6% of the total glacier-covered area (Fig. 3C).

The majority of glaciers on Nanga Parbat are located on NW- to NE-facing slopes. However, in the Rupal Valley, most glaciers are exposed to directions ranging from S to NW (Fig. 3B) mainly because of the vertical extent of the Rupal Wall (Fig. 2). Taking into account the entire massif, most glaciers are situated at altitudes higher than 4000 m a.s.l. with almost 50% of the ice-covered area in the elevation range between 4000 and 5500 m a.s.l. (Fig. 3D). Only 14 valley glaciers with almost completely debris-covered tongues reach altitudes below 4000 m a.s.l., with Chungphare Glacier showing the lowest minimum elevation at about 2910 m a.s.l. The median elevation of these 14 glaciers varies between approximately 4000 m a.s.l. (Sachen) and

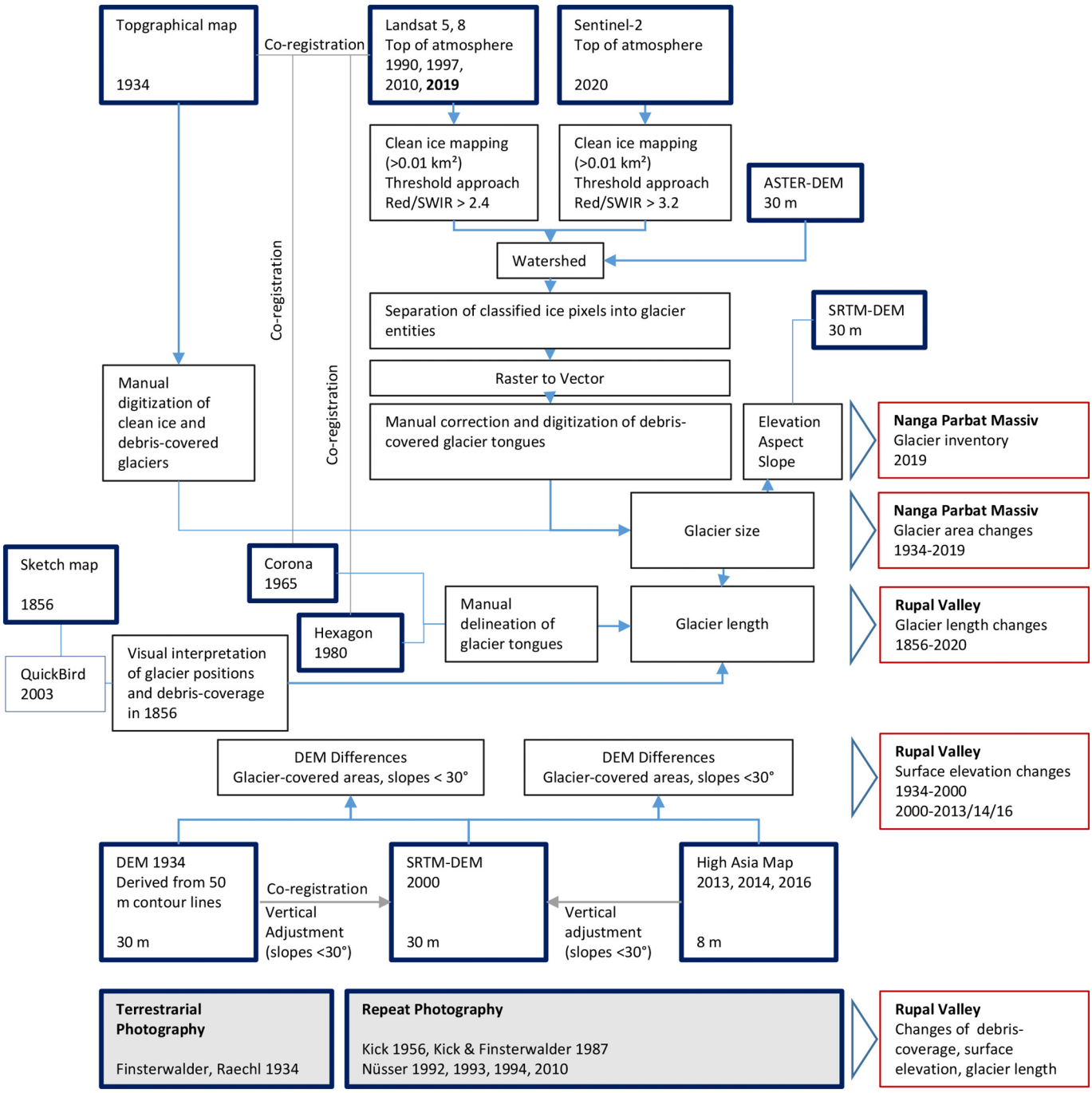

Fig. 2. Workflow showing the data and methodology conducted in order to investigate the distribution of glaciers and glacier area changes in the Nanga Parbat region and to analyse glacier length and surface changes in the Rupal Valley.

6000 m a.s.l. (Shaigiri). One of them has an altitudinal range of just 1980 m (Harcho), whereas eight exceed 3000 m, with a maximum of 4760 m (Bizhin). The large altitudinal range of these glaciers underlines the importance of snow and ice re-distribution through avalanches. The mean slope angle of all glaciers is 28° and varies between 14° and 46°; the mean slope angle of three glaciers larger than 10 km^2 even exceeds 30°. The debris-covered glacier tongues are located on slopes of less than 10°; whereas the clean ice parts are usually characterised by steeper slopes (Fig. 3E, F). The longitudinal profiles of all large valley glaciers around the Nanga Parbat massif indicate the characteristic features of "Mustagh" and "Turkestan" types with steep slopes, large vertical extent and gently sloped glacier tongues; only the Rupal Glacier belongs to the "Alpine" type (Fig. 3G).

4.2. Glacier changes

The area change detection of 63 glaciers mapped on the 1934-toposheet and satellite imagery from 2019 indicates that the ice covered area decreased from about 243 km^2 to 225.9 ± 10.6 km^2 by 7% (0.1% yr^{-1}) and three glaciers disappeared completely. Likewise, the analysis of all glaciers larger than 0.01 km^2 in the entire study area indicates only a small shrinkage of 4% (0.2% yr^{-1}) from 313.0 ± 24.3 km^2 in 1990 to 299.7 ± 24.1 km^2 in 2019. The annual decreasing rate varies between 0.2% yr^{-1} from 1990 to 1997 (309.3 ± 24.3 km^2), 0.1% yr^{-1} from 1997 to 2013 (305.8 ± 23.9 km^2), and 0.3% yr^{-1} (299.6 ± 24.1 km^2) from 2013 to 2019. In total, the detected glacier changes are within the range of uncertainty and only a slight decrease or stable conditions

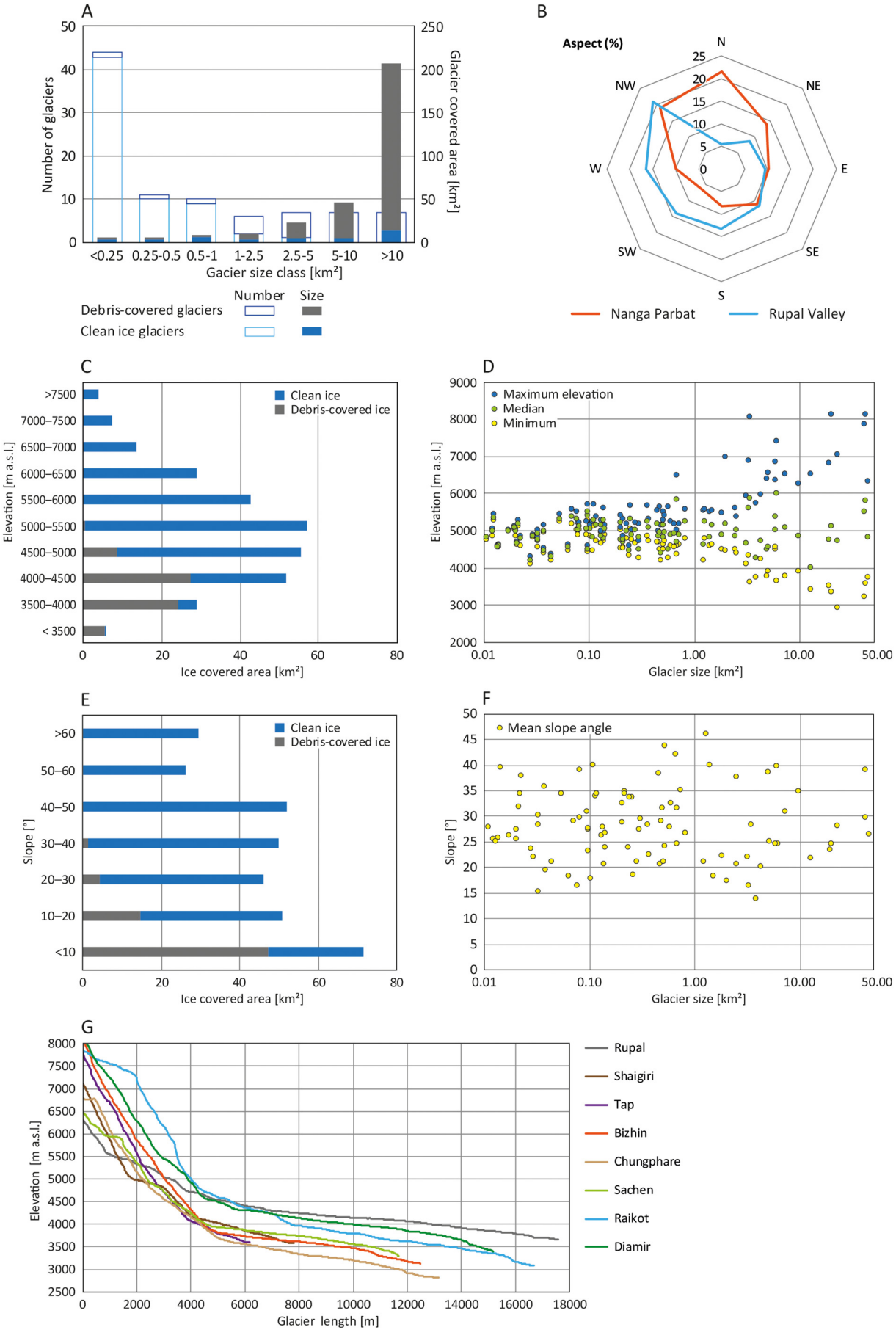
A
Number of glaciers
Glacier covered area [km²]
<0.25 0.25-0.5 0.5-1 1-2.5 2.5-5 5-10 >10
Gacier size class [km²]
Number Size
Debris-covered glaciers
Clean ice glaciers
B
Aspect (%)
N NE E SE S SW W NW
Nanga Parbat
Rupal Valley
C
Clean ice
Debris-covered ice
Elevation [m a.s.l.]
>7500 7000–7500 6500–7000 6000–6500 5500–6000 5000–5500 4500–5000 4000–4500 3500–4000 < 3500
Ice covered area [km²]
D
Maximum elevation
Median
Minimum
Elevation [m a.s.l.]
Glacier size [km²]
E
Clean ice
Debris-covered ice
Slope [°]
>60 50–60 40–50 30–40 20–30 10–20 <10
Ice covered area [km²]
F
Mean slope angle
Slope [°]
Glacier size [km²]
G
Elevation [m a.s.l.]
Glacier length [m]
Rupal
Shaigiri
Tap
Bizhin
Chungphare
Sachen
Raikot
Diamir

can be identified. Between 1934 and 2019 the relative debris-coverage area increased from 15 to 21% in 1990 and to 23% in 2019.

Taking all individual ice-bodies into consideration, the average change amounts to −23% (−0.8% yr^{-1}) over the observation period between 1990 and 2019. It varies from −0.2% yr^{-1} between 1990 and 1997 to −0.1% yr^{-1} between 1997 and 2013 and −0.3% yr^{-1} between 2013 and 2019 (Fig. 4). In the size classes smaller than 0.5 km^2 the average glacier change amounts to −33% (−1.2% yr^{-1}), which is significantly higher compared to glaciers larger than 1 km^2 with an average change of about −5% (−0.2% yr^{-1}). For only the debris-covered glaciers, the average decrease is −3% (−0.1% yr^{-1}).

4.3. Glaciers in the Rupal Valley

A series of largely avalanche-fed glaciers on the South Face of Nanga Parbat can be found in the Rupal Valley. The largest are the glaciers Chungphare, Bizhin, Tap, and Shaigiri. Only the Rupal Glacier originating from the Toshain Peak (6270 m a.s.l.) and the Laila Peak (5971 m a.s.l.) can be characterised as an "Alpine" type glacier. The 1856-sketch map by Schlagintweit (Kick, 1967; Nüsser, 2015) enables the extension of the observation period of glacier changes to the last 164 years.

4.3.1. Chungphare Glacier

The Chungphare Glacier shows the characteristics of a "Mustagh" type glacier and covered an area of about 23.3 ± 2.0 km^2 in 2019. It has changed from 23.4 km^2 in 1934 to 24.2 ± 2.1 km^2 in 1990 and to 23.3 ± 2.0 km^2 in 2019 (−3.6% between 1990 and 2019). This glacier ranges in altitude from about 2910 m a.s.l. to 7030 m a.s.l. with a median elevation of 4690 m a.s.l. and a mean slope angle of 28°. It consists of two main ice-streams with a confluence at about 3300 m a.s.l. and some small tributary glaciers along the west-facing slope. About 24% of the glacier and its tributaries was debris-covered in 2019. The sketch map and corresponding landscape paintings from 1856 indicate a higher glacier surface with clean ice and only small debris-covered strips along both sides. The interface between debris-covered and clean ice at Chungphare Glacier increased to an altitude of 3580 m a.s.l. in 1934 and up to 3700 m a.s.l. in 2020. The characteristic glacier surface structures with ogives on the orographic right ice stream (Fig. 2 in Data in Brief) can also be seen in the 1856 sketch map (Fig. S2a). At that time, the Chungphare Glacier reached down to the curve of the Rupal River at the confluence with a tributary stream and the tongue was bounded by a rocky ridge and the lateral moraine, which dammed a meltwater lake that caused several outburst floods (Drew, 1875; Neve, 1907; Schlagintweit, 1872). Reports of historical fluctuations of Chungphare Glacier include shrinking of the less-crevassed clean ice surface by around 30 m after a lake outburst (Drew, 1875) and rapid glacier advance by about 90 m between 1887 and 1906 (Neve, 1907). Due to the glacier blockage by the ridge, only a small part of the ice tongue moved further downstream. Including this lobe, a total glacier retreat of about 1000 m can be reconstructed between 1856 and 2020 (6.6 m yr^{-1}). The glacier tongue advanced and retreated several times with a total retreat of about 780 m (9.8 m yr^{-1}) between 1856 and 1934 and about 220 ± 41 m (2.6 ± 0.5 m yr^{-1}) between 1934 and 2020. By 1987 the lobe had retreated back to the ridge (280 m) with a rate of 5.3 m yr^{-1} (2.9 m yr^{-1} in 1934–1958 to 7.2 m yr^{-1} in 1958–1987) (Kick, 1994; Fig. 3 in Data in Brief). While the glacier tongue was still in contact with the ridge in 1980, the runoff of Rupal River took place via a subglacial tunnel and the glacier front retreated by 120 ± 42 m (12 ± 4.2 m yr^{-1}) between 1980 and 1990. Collapse of the glacier snout above the river occurred in 1985 (Kick, 1994), resulting in the higher retreat for that decade. Since 1990 the glacier front is stable

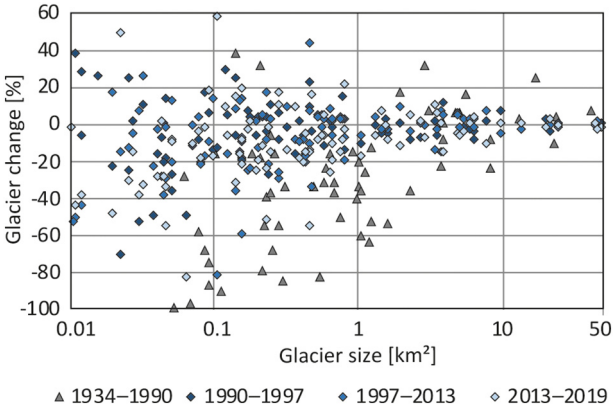

Fig. 4. Glacier area changes in relation to size over different observation periods.

and a slight advance of about 35 ± 44 m (5 ± 6.2 m yr^{-1}) can be detected for the period between 2013 and 2020 (Fig. 5).

Observations by Schlagintweit suggest a position of the glacier surface around 20 m below the moraine crest in 1856 with further downwasting at a rate of about 0.31 m yr^{-1} between 1856 and 1934 (Kick, 1994). Multitemporal repeat photography from a viewpoint on the orographic right moraine proves continuous volume loss between 1934 and 1987 but a noticeable volume increase between 1987 and 2010 (Fig. 4 in Data in Brief). These findings are in line with measurements at this profile based on remote sensing data and GPS data taken during our own field survey in 2010. Additional ice velocity measurements confirm a surging event of Chungphare Glacier in 2005 and 2006 (Mack, 2019). The surface difference amounts to 22 ± 34 m between 1934 and 2000 while the lowering rate has only slightly increased to 0.3 ± 0.5 m yr^{-1} between 2000 and 2016. During this period the glacier surface was dissected, with no significant vertical changes in the centre of the glacier and downwasting on both sides. Moraine ridges and different sliding moraines can be detected on both sides of Chungphare glacier (Fig. S3a, Fig. 6). For the entire glacier tongue (slope angle <30°) the mean surface lowering amounts to 17 ± 34 m (0.3 ± 0.5 m yr^{-1}) between 1934 and 2000 and to 2 ± 7 m (0.1 ± 0.4 m yr^{-1}) between 2000 and 2016; in both observation periods, the highest downwasting rates can be observed above the confluence of both glacier tongues (Fig. S3b).

4.3.2. Bizhin Glacier

The Bizhin Glacier can be characterised as a "Turkestan" type glacier and covers an area of about 20.2 ± 1.6 km^2 in 2019. Its ice-covered area changed from 16.9 km^2 in 1934 to 21.0 ± 1.4 km^2 in 1990 and to 20.2 ± 1.6 km^2 in 2019 (−3.7% between 1990 and 2019). It ranges in altitude from 3340 m a.s.l. to the summit at 8126 m a.s.l. with a median elevation of about 5110 m a.s.l. and a mean slope angle of 25°. The upper glacier catchment is characterised by steep rock walls and connected to the main tongue by three ice streams; which act as avalanche tracks. Avalanche deposits detected for six separate years always cover areas of more than 2 km^2 at an altitude of about 3900 m a.s.l. in the runout zone, while their starting zone can be located up to 3000 m higher (Fig. 7). The avalanche runout zone in the upper portion of the glacier tongue (*Firnkessel* literal meaning firn caldron) is also shown as free of debris-cover in the sketch map by Schlagintweit (Fig. S2b). The entire Bizhin Glacier has a debris cover of just 26%. However, the tongue is completely debris-covered (Fig. 5 in Data in Brief).

Fig. 3. Glacier inventory of the entire Nanga Parbat massif for the year 2019. Glacier size classes (A); aspect of glaciers and glacier-covered area (B); elevation range of glacierized area differentiated between clean ice and debris-covered area (C); minimum and maximum elevation per glacier (D); slope of glacierized area differentiated between clean ice and debris-covered area (E); mean slope angle per glacier (F); and longitudinal profiles of large valley glaciers (G).

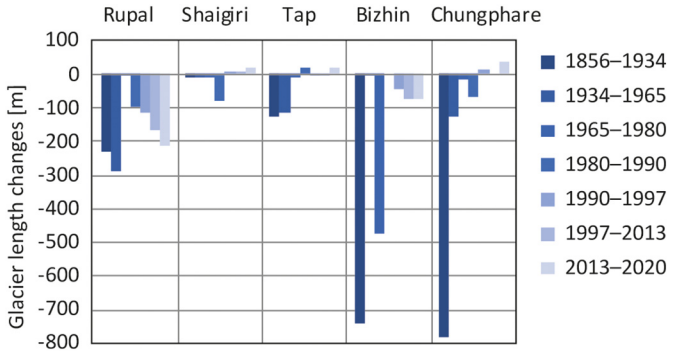

Fig. 5. Changes of glacier length in the Rupal Valley.

The total retreat of Bizhin Glacier amounts to about 1400 m (11.2 m yr^{-1}) over the whole observation period. A glacier advance between 1856 and 1895 can be assumed, since the snout position in the 1856-sketch map does not fit with satellite data and field observations by Collie (1897, 1902) suggest a glacial maximum in 1895 when he describes the glacier surface to be "flush with the top of the moraine". Therefore, it is not possible to quantify changes in the second half of the 19th century. While a front retreat of about 740 m (19 m yr^{-1}) can be derived for the period between 1895 and 1934, a lower retreat of 663 ± 41 m (7.7 ± 0.5 m yr^{-1}) can be detected between 1934 and 2020. The glacier tongue remained stable during the period between 1934 and 1965 and decreased by about 474 ± 42 m (19.0 ± 1.7 m yr^{-1}) until 1990. Our own field observations indicate that the right part of the glacier tongue is tunnelled by the main Rupal River and partial glacier collapse similar to the Chungphare Glacier might have caused this higher retreat. The snout position shows only slight retreat with 6.3 ± 7.8 m yr^{-1} (1990–1997) and 4.5 ± 4.3 m yr^{-1} (1997–2013), confirmed by repeat photography (Fig. 6 in Data in Brief). A slightly higher decrease is detectable with about 10.3 ± 0.4 m yr^{-1} for the latest period (2013−2020). Thinning of Bizhin Glacier amounts to 18 ± 34 m (0.3 ± 0.5 m yr^{-1}) between 1934 and 2000, which is identical to the thinning rates calculated by Kick (1994) for the period between 1934 and 1958 amounting to an average of 5.5 m for the glacier tongue between 3400 and 4300 m a.s.l. Another 2 m ± 6.9 m of glacier thinning between 2000 and 2013 (0.1 ± 0.5 m yr^{-1}) is within the range of uncertainty (Fig. S3c). A slight mass gain in the lower part can be detected (Fig. 7 in Data in Brief). Contrary to the assessment by Kick (1994) that there are no surge events on the glaciers of Nanga Parbat, Mack (2019) detected active surging phases for both Bizhin and Chungphare glaciers in 2005 and 2006. This finding is confirmed by a recent study by Muhammad et al. (2019b) who identify ice thickening in some sections of the Bizhin Glacier.

4.3.3. Tap Glacier

The Tap Glacier has an altitudinal range of 3610 to 8020 m a.s.l. with a median elevation of 5840 m a.s.l. and a mean slope angle of 28°. It covered an area of 3.5 ± 0.5 km^2 in 2019 and the debris-cover amounted to 17%. This glacier is located on a pedestal moraine with a proglacial lake (size 0.08 km^2), which is located about 50 m above the valley floor. The 1934 toposheet shows a glacier size of 2.9 km^2, whereas it amounts to 3.8 ± 0.4 km^2 in 1990 and decreased by about 8% to 3.5 ± 0.5 km^2 in 2019, which is within the range of uncertainty. Regarding the glacier length changes, a potential retreat rate between 1856 and 1934 cannot be estimated, since it is not clear, if an initial moraine dammed lake already existed in 1856. The glacier tongue seems to be stable and shows only a minor retreat of 103 ± 41 m between 1934 and 2020 (1.2 ± 0.5 m yr^{-1}). No changes of the surface are detectable in satellite imagery between 2000 and 2013 and in repeat photography between 1993 and 2010 (Fig. 8 in Data in Brief). According to the cross-sections, only a small gap between the moraine and the ice surface exist, thus minor thinning can be assumed although the estimated downwasting between 1934 and 2013 amounts to about 20 m (Fig. S3e).

4.3.4. Shaigiri Glacier

The Shaigiri Glacier is another pedestal glacier with a characteristic curve towards the east, which is probably caused by a former larger main Rupal Glacier from the Last Glacial Maximum. It is characterised by a debris-covered tongue (22% of the total glacier) and an avalanche-fed *Firnkessel* at about 5000 m a.s.l. (Fig. S1). In 1934 the glacier was mapped with an area of 5.5 km^2. The glacier size decreased from 6.4 ± 0.6 km^2 in 1990 to 6.0 ± 0.6 km^2 in 2013 and increased to 6.2 ± 0.6 km^2 in 2019. Considering glacier length changes, the total retreat of the Shaigiri Glacier is estimated to 93 m between 1856 and 2020. As on the sketch map by Schlagintweit, a small gap between the glacier and the stream exists which is intersected by two small glacial rivulets. After a long stable period, which lasted from 1856 to 1980, the glacier retreated by about 80 m between 1980 and 1990. Since then the glacier is stable. The photographs show the formation of a small supraglacial lake between 1934 and 1987 and a second small lake in close proximity between 1993 and 2010, both dammed by the terminal moraine (Fig. 9 in Data in Brief). Own observations in the 1990s and in 2010 as well as the comparative analysis of DEMs (Fig. 6d) show that the glacier surface matches with the lateral moraine.

4.3.5. Rupal Glacier

The "Alpine" type Rupal Glacier is located at the valley head and forms the largest glacier in the entire Nanga Parbat region. As only the eastern part of the glacier tongue is shown on the 1:50,000 toposheet from 1934, comparative analyses have to be based on the map at the scale of 1:100,000, which was produced by the same expedition. The glacier area decreased from 51.9 km^2 in 1934 to 48.2 ± 2.1 km^2 in 1990 and to 46.1 ± 2.2 km^2 in 2019 (7% between 1934 and 1990 and 4% between 1990 and 2019). Unlike all other glaciers of the Rupal Valley, this ice stream is not predominantly avalanche-fed. It ranges from 3730 m to 6300 m a.s.l. and its tongue is fed by two branches, which merge at 4150 m a.s.l. Schlagintweit mapped this glacier with its characteristic medial moraine and two strips of clean ice reaching about 2.8 km further below compared to 2020 (Fig. S2c). This massive retreat becomes also visible by repeat photography between 1934 and 2010 (Figs. 10, 11 and 12 in Data in Brief) while the debris-covered portion of the glacier increased from 15% to 23% between 1934 and 2019.

A total retreat of 1.1 km can be estimated over the entire observation period between 1856 and 2020. Unlike the other ice bodies, the Rupal Glacier shows increasing retreat rates since 1934. While the retreat amounted to 228 m (2.9 m yr^{-1}) for the period between 1856 and 1934, it increased to 885 ± 41 m (10.3 ± 0.5 m yr^{-1}) for the interim 1934–2020. The highest retreat rate was detected for the period 2013–2020 with 211 ± 44 m (30.2 ± 6.2 m yr^{-1}).

The Rupal Glacier is also characterised by a massive loss in volume, especially in its lower part (Fig. 6e). Corresponding to the drastic retreat, the surface thinning amounts to 38 ± 34 m (0.6 ± 0.5 m yr^{-1}) between 1934 and 2000 for the glacier tongue below 4200 m a.s.l. shown on the 1934-toposheet. The almost completely debris-covered lower tongue melted down by another 22 ± 7 m (1.6 ± 0.5 m yr^{-1}) between 2000 and 2014 (Fig. 6d). This massive downwasting of about 40 m between the glacier surface and the crest of the lateral moraines is confirmed by our own GPS data from 2010 at an altitude of about 4000 m a.s.l. However, the average surface lowering for the entire glacier (<30°) amounts to 7 ± 7 m (0.5 ± 0.5 m yr^{-1}), without taking into account the higher penetration of radar data compared to optical data.

5. Discussion

This study shows the high potential and the limitations of multi-temporal and multi-source approaches to investigate glacier changes

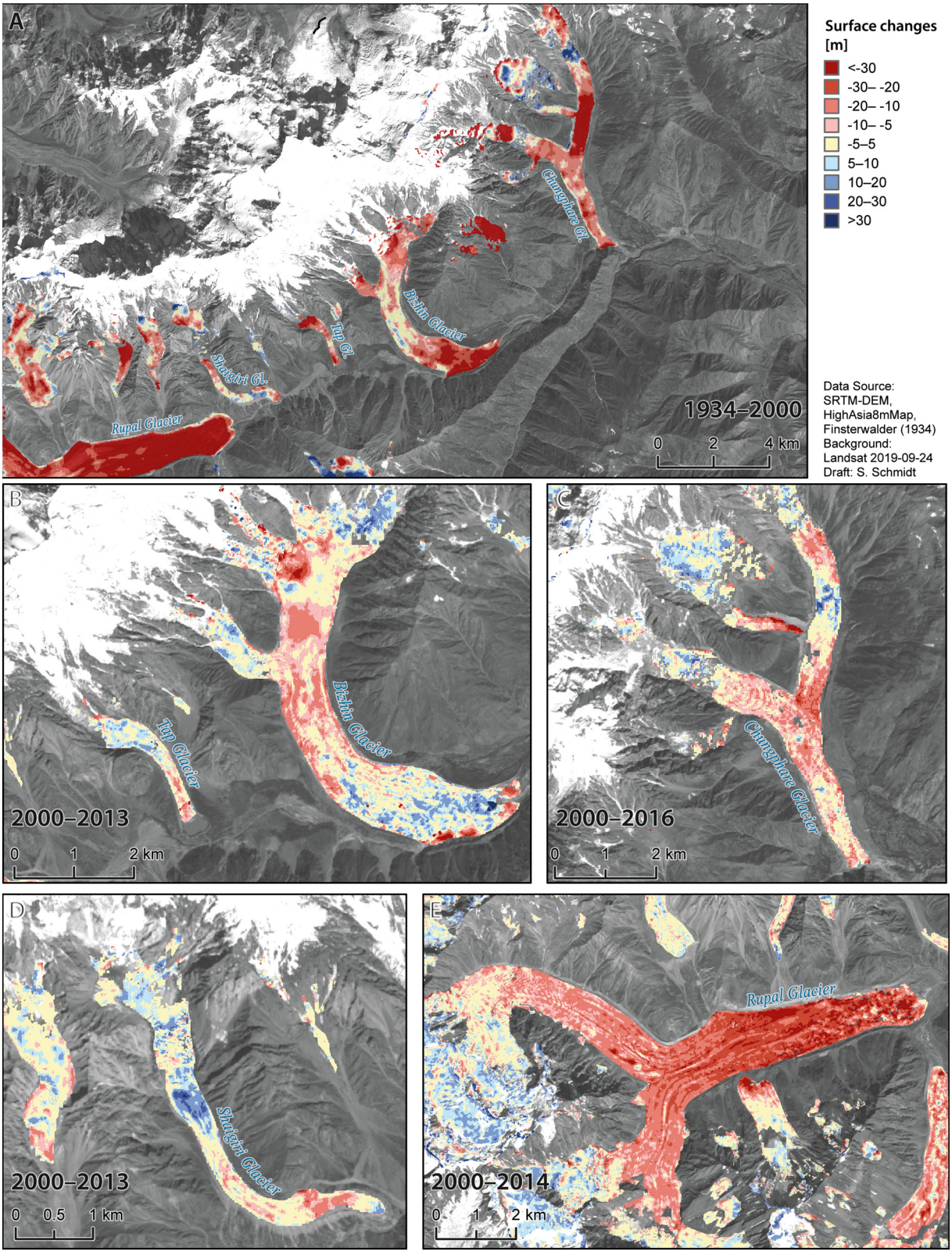

Fig. 6. Differences of surface elevation between 1934 and 2000 (A), Bizhin and Tap Glacier between 2000 and 2013 (B), Chungphare Glacier between 2000 and 2016 (C), Shaigiri Glacier between 2000 and 2013 (D), and Rupal Glacier between 2000 and 2014 (E).

over long observation periods. In addition to often observed planimetric shifts (Bhambri and Bolch, 2009), some areas of the 1934 toposheet from Nanga Parbat have to be excluded from analysis as the detected differences between the map and satellite imagery are too large (Spohner, 2004). While comparisons between the historical toposheet and satellite images show a high congruence in the glacier tongues, larger differences become evident between steep rock slopes and wall glaciation at higher altitudes, resulting in difficulties in estimating

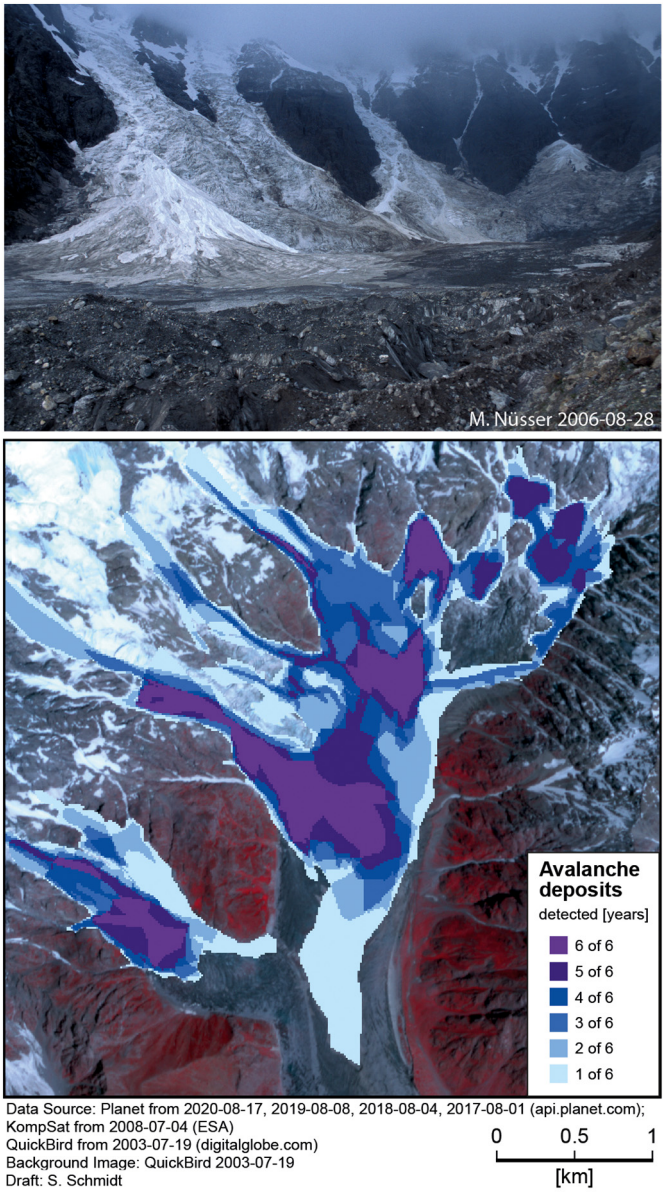

Fig. 7. The avalanche runout zone of Bizhin Glacier shows the importance of re-distributed snow for glacier nourishing. The map indicates several avalanche deposits in six years. In the photograph from August 2006 the different ages of avalanche cones are visible.

changes in total glacier sizes. Multi-temporal mapping exercises need to consider an overestimation of ice-free areas and corresponding underestimation of ice coverage on the 1934 toposheet compared to the satellite data. This might be caused by distinctive differences in viewing angles between terrestrial photogrammetry from opposite slopes in the case of the 1934 map and the near vertical perspective of satellite sensors. Furthermore, snow accumulation along rock spurs and couloirs regularly results in mixed pixels that may lead to an overestimation of ice on steep walls. Despite the relatively high threshold of 2.4 (in many studies a threshold of 2.0 is recommended, e.g. Racoviteanu et al., 2009), these rock slopes are classified as ice. While the contour lines show high accuracy in most parts of the 1934 toposheet, some areas are characterised by large discrepancies, which are either caused by the interpolation algorithm to generate the DEM from contour lines (Spohner, 2004) or by mapping errors in the toposheet. As the elevation differences show an irregular spatial pattern a systematic error can be excluded for the case of Nanga Parbat.

Similar to other Himalayan regions, this glacier inventory shows that the majority of glaciers are smaller than 1 km^2 but contribute only to about 10% of the total glacier-covered area. With a mean size of 3.1 km^2, the glaciers of the Nanga Parbat massif are much larger than those in the Shyok Valley (1.4 km^2) in the eastern Karakoram (Bhambri et al., 2013). The relative debris-coverage of glaciers in the Nanga Parbat region amounts to 24%, which is higher than that for other parts of the UIB (Khan et al., 2015). For the entire Himalayan arc, estimates of debris-covered glacier area vary between 10% and 25% (Bolch et al., 2019).

Both the size and the debris-cover have a strong impact on glacier changes (Cogley, 2016; Hewitt, 2014). The observed shrinkage rate of the glacier-covered area on the Nanga Parbat (0.15% yr^{-1} for the period 1990–2019) is considerably lower than the glacier decrease in the Nanda Devi region, where 0.27% yr^{-1} is reported for the period 1980–2017 (Kumar et al., 2021) or in the Khumbu Himalaya of Nepal, where the same annual percentage was detected for the timespan 1962–2011 (Thakuri et al., 2014). In the Suru sub-basin of Zanskar in the eastern proximity of the Nanga Parbat region, the glacier covered area decreased with a rate of 0.13% yr^{-1} from 1971 to 2017 (Shukla et al., 2020). In the same line Bhambri et al. (2013) identified insignificant glacier area changes in the Shyok Valley between 1973 and 2011.

As observed in different Himalayan regions small glaciers are characterised by a higher average decrease than larger ones (Bhambri et al., 2011; Bolch et al., 2019; Cogley, 2016). Taking into consideration only debris-covered glaciers, the mean shrinkage rate is significantly lower. Thus, low observed shrinkage rates in the Karakoram and in the Nanga Parbat region are partly caused by the thick debris-cover which protects the glacier tongues (Hewitt, 2011). However, the debris-covered Zemu Glacier to the east of the Kangchenjunga massif in the Eastern Himalaya has shrunk by about 0.25% yr^{-1} since 1931 (Rashid and Majeed, 2020). The impacts of thin debris-cover (Hewitt, 2014; Muhammad et al., 2020) and ice cliffs (Brun et al., 2016) on melting rates are still under discussion.

Overall, the debris-covered large valley glaciers of the Nanga Parbat region show only small surface lowering rates. Similar observations have been published by Zhou et al. (2017), who found slightly negative mass balances for the Karakoram glaciers between the 1970s and 2000 with a heterogenous pattern in space and time and by Soheb et al. (2020), who studied the Stok Glacier in the Trans-Himalaya of Ladakh between 1978 and 2019. In the study area of Rupal Valley, all large valley glaciers originating from the Rupal Wall are predominantly fed by avalanches over long distances are characterised by low retreating rates. In contrast, the Rupal Glacier, which is not primarily avalanche-fed shows higher retreat rates. Together with the steep altitudinal climatic gradients (Winiger et al., 2005), this verticality effect (Hewitt, 2014, 2011) plays an important role on mass balances. Therefore, further investigations on the role of avalanches are needed for an improved understanding of glacier changes. Furthermore, different response patterns of individual glaciers are partly caused by surge events, as detected in the cases of Chungphare and Bizhin (Mack, 2019; Muhammad et al., 2019b). In contrast to the fluctuations of Raikot Glacier (Schmidt and Nüsser, 2009), or surge events in the Karakoram (Bhambri et al., 2017), no larger frontal movements of glaciers can be detected in the Rupal Valley. In some cases site-specific factors such as the position of ridges or subglacial tunnelling of main rivers need to be considered to explain periods with higher glacier retreat rates.

6. Conclusion

The glaciers of Nanga Parbat show a slight but continuous decrease and an increased debris-cover since 1856, when Adolph Schlagintweit mapped them for the first time. The massif is characterised by its transitional position between the Karakoram and the Himalaya and can therefore be interpreted as the southernmost part of the 'Karakoram Anomaly' (Hewitt, 2005). Nanga Parbat is well suited for the study of Himalayan glacier changes because of the large multi-temporal data base. This study demonstrates the potential of combining multiple

sources and the relevance of field-based and historically contextualized research at a local scale. However, it also shows the challenges in transforming multiple forms of data such as maps, photographs and remote sensing imagery into a standardized form for comparison. Moreover, the integration of geophysical methods such as Ground Penetrating Radar to estimate ice volumes and the use of proxies such as dendrochronological and pedological data for detailed chronologies of glacier retreat offers a fruitful direction for future studies.

CRediT authorship contribution statement

Marcus Nüsser: Conceptualization, Methodology, Formal analysis, Investigation, Writing – original draft, Writing – review & editing, Data curation, Project administration. **Susanne Schmidt:** Conceptualization, Methodology, Formal analysis, Investigation, Writing – original draft, Writing – review & editing, Data curation.

Declaration of competing interest

The authors declare that they have no known competing financial interests or personal relationships that could have appeared to influence the work reported in this paper.

Acknowledgement

Fieldwork for this project was funded by the German Research Foundation (DFG) in the context of the Culture Area Karakoram during the 1990s and by Heidelberg University in the years 2006 and 2010. We thank Akhtar Hussain (Tarishing, Gilgit) for his continuous support on all field surveys between 1992 and 2010. We are grateful to the European Space Agency (ESA), the United States Geological Survey (USGS) and PlanetScope for providing satellite imagery. Earlier versions of this research have been presented at the EGU General Assembly and other international conferences. We also thank the three anonymous reviewers for their comments and suggestions as well as Dr. Ravi Baghel (Heidelberg) for careful proof-reading.

Appendix A. Supplementary data

Supplementary data to this article can be found online at https://doi.org/10.1016/j.scitotenv.2021.147321.

References

Bhambri, R., Bolch, T., 2009. Glacier mapping: a review with special reference to the Indian Himalayas. Prog. Phys. Geogr. 35 (3), 672–704. https://doi.org/10.1177/0309133309348112.

Bhambri, R., Bolch, T., Chaujar, R.K., Kulshreshtha, S.C., 2011. Glacier changes in the Garhwal Himalaya, India, from 1968 to 2006 based on remote sensing. J. Glaciol. 57, 543–556. https://doi.org/10.3189/002214311796905604.

Bhambri, R., Bolch, T., Kawishwar, P., Dobhal, D.P., Srivastava, D., Pratap, B., 2013. Heterogeneity in glacier response in the upper Shyok valley, northeast Karakoram. Cryosphere 7, 1385–1398. https://doi.org/10.5194/tc-7-1385-2013.

Bhambri, R., Hewitt, K., Kawishwar, P., Pratab, B., 2017. Surge-type and surge-modified glaciers in the Karakoram. Sci. Rep. 7 (1), 1–14. https://doi.org/10.1038/s41598-017-15473-8.

Bolch, T., Menounos, B., Wheate, R., 2010. Landsat-based inventory of glaciers in western Canada, 1985–2005. Remote Sens. Environ. 114, 127–137. https://doi.org/10.1016/j.rse.2009.08.015.

Bolch, T., Kulkarni, A., Kääb, A., Huggel, C., Paul, F., Cogley, J.G., Frey, H., Kargel, J.S., Fujita, K., Scheel, M., Bajracharya, S., Stoffel, M., 2012. The state and fate of Himalayan glaciers. Science 336 (6079), 310–314. https://doi.org/10.1126/science.1215828.

Bolch, T., Shea, J.M., Liu, S., Azam, F.M., Gao, Y., Gruber, S., Immerzeel, W.W., Kulkarni, A., Li, H., Tahir, A.A., Zhang, G., Zhang, Y., 2019. Status and change of the cryosphere in the extended Hindu Kush Himalaya Region. In: Wester, P., Mishra, A., Mukherji, A., Shrestha, A.B. (Eds.), The Hindu Kush Himalaya Assessment: Mountains, Climate Change, Sustainability and People. Springer International Publishing, Cham, pp. 209–255 https://doi.org/10.1007/978-3-319-92288-1_7.

Brun, F., Buri, P., Miles, E.S., Wagnon, P., Steiner, J., Berthier, E., et al., 2016. Quantifying volume loss from ice cliffs on debris-covered glaciers using high-resolution terrestrial and aerial photogrammetry. J. Glaciol. 62 (234), 684–695. https://doi.org/10.1126/science.1215828.

Byers, A.C., 2000. Contemporary landscape change in the Huascaran National Park and buffer zone, Cordillera Blanca, Peru. Mt. Res. Dev. 20 (1), 52–63. https://doi.org/10.1659/0276-4741(2000)020[0052:CLCITH]2.0.CO;2.

Byers, A.C., 2007. An assessment of contemporary glacier fluctuations in Nepal's Khumbu Himal using repeat photography. Himal. J. Sci. 4 (6), 21–26.

Chand, P., Sharma, M.C., Bhambri, R., Sangewar, C.V., Juyal, N., 2017. Reconstructing the pattern of the Bara Shigri glacier fluctuation since the end of the Little Ice Age, Chandra valley, north-western Himalaya. Prog. Phys. Geogr. 41 (5), 643–675. https://doi.org/10.1177/0309133317728017.

Cogley, J.G., 2011. Present and future states of Himalaya and Karakoram glaciers. Ann. Glaciol. 52 (59), 69–73. https://doi.org/10.3189/172756411799096277.

Cogley, J.G., 2016. Glacier shrinkage across High Mountain Asia. Ann. Glaciol. 57 (71), 41–49. https://doi.org/10.3189/2016AoG71A040.

Collie, J.N., 1897. Climbing on the Nanga Parbat range, Kashmir. Alp. J. 19, 17–32.

Collie, J.N., 1902. Climbing on the Himalaya and Other Mountain Ranges. D. Douglas, Edinburgh.

Copland, L., Sylvestre, T., Bishop, M.P., Shroder, J.F., Seong, Y.B., Owen, L.A., Bush, A., Kamp, U., 2011. Expanded and recently increased glacier surging in the Karakoram. Arct. Antarct. Alp. Res. 43 (4), 503–516. https://doi.org/10.1657/1938-4246-43.4.503.

Dahri, Z. H., Ludwig, F., Moors, E., Ahmad, B., Khan, A., Kabat, P., 2016. An appraisal of precipitation distribution in the high-altitude catchments of the Indus basin. Sci. Total Environ. 548–549, 289–306. doi:https://doi.org/10.1016/j.scito tenc.2016.01.001.

Dickoré, W.B., Nüsser, M., 2000. Flora of Nanga Parbat (NW Himalaya, Pakistan): an annotated inventory of vascular plants with remarks on vegetation dynamics. Englera 19, 3–253. https://doi.org/10.2307/3776769.

Drew, F., 1875. The Jummoo and Kashmir Territories. A Geographical Account. E. Stanford, London.

Dwyer, J.L., Roy, D.P., Sauer, B., Jenkerson, C.B., Zhang, H.K., Lymburner, L., 2018. Analysis ready data: enabling analysis of the Landsat archive. Remote Sens. 10, 1363. https://doi.org/10.3390/rs10091363.

Eckerstorfer, M., Bühler, Y., Frauenfelder, R., Malnes, E., 2016. Remote sensing of snow avalanches: recent advances, potential, and limitations. Cold Reg. Sci. Technol. 121, 126–140. https://doi.org/10.1016/j.coldregions.2015.11.001.

Farhan, S.B., Zhang, Y., Ma, Y., Guo, Y., Ma, N., 2015. Hydrological regimes under the conjunction of westerly and monsoon climates: a case investigation in the Astore Basin, northwestern Himalaya. Clim. Dyn. 44 (11), 3015–3032. https://doi.org/10.1007/s00382-014-2409-9.

Farinotti, D., Immerzeel, W.W., de Kok, R.J., Quincey, D.J., Dehecq, Amaury, 2020. Manifestations and mechanisms of the Karakoram glacier anomaly. Nat. Geosci. 13, 8–16. https://doi.org/10.1038/s41561-019-0513-5.

Finsterwalder, R., 1937. Die Gletscher des Nanga Parbat. Glaziologische Arbeiten der Deutschen Himalaya-Expedition 1934 und ihre Ergebnisse. Z. Gletscherk. 25, 57–108.

Finsterwalder, R., 1938. Die geodätischen, gletscherkundlichen und geographischen Ergebnisse der deutschen Himalaja Expedition 1934 zum Nanga Parbat. Siegismund, Berlin.

Gardelle, J., Berthier, E., Arnaud, Y., 2012. Slight mass gain of Karakoram glaciers in the early twenty-first century. Nat. Geosci. 1450. https://doi.org/10.1038/NGEO1450.

Gardelle, J., Berthier, E., Arnaud, Y., Kääb, A., 2013. Region-wide glacier mass balances over the Pamir-Karakoram-Himalaya during 1999–2011. Cryosphere 7 (4), 1263–1286. https://doi.org/10.5194/tc-7-1263-2013.

Gardent, M., Rabatel, A., Dedieu, J.P., Deline, P., 2014. Multitemporal glacier inventory of the French Alps from the late 1960s to the late 2000s. Glob. Planet. Chang. 120, 24–37. https://doi.org/10.1016/j.gloplacha.2014.05.004.

Gardner, J.S., 1986. Recent fluctuations of Rakhiot glacier, Nanga Parbat, Punjab Himalaya, Pakistan. J. Glaciol. 32, 527–529. https://doi.org/10.1017/S0022143000012247.

Granshaw, F.D., Fountain, A.G., 2006. Glacier change (1958–1998) in the North Cascades National Park complex, Washington, USA. J. Glaciol. 52(177), 251–256. doi:https://doi.org/10.3189/172756506781828782.

Hewitt, K., 2005. The Karakoram anomaly? Glacier expansion and the 'elevation effect', Karakoram Himalaya. Mt. Res. Dev. 25 (4), 332–340. https://doi.org/10.1659/0276-4741(2005)025[0332:TKAGEA]2.0.CO;2.

Hewitt, K., 2007. Tributary glacier surges: an exceptional concentration at Panmah Glacier, Karakoram Himalaya. J. Glaciol. 53 (181), 181–188. https://doi.org/10.3189/172756507782202829.

Hewitt, K., 2011. Glacier change, concentration, and elevation effects in the Karakoram Himalaya, Upper Indus Basin. Mt. Res. Dev. 31 (3), 188–200. https://doi.org/10.1659/MRD-JOURNAL-D-11-00020.1.

Hewitt, K., 2014. Glaciers of the Karakoram Himalaya: Glacial Environments, Processes, Hazards and Resources. Springer, Dordrecht; Heidelberg.

Hock, R., Rasul, G., Adler, C., Cáceres, S.Gruber, Hirabayashi, M.Jackson, Kääb, S.Kang, Kutuzov, S., Milner, U.Molau, Morin, S., Orlove, H.Steltzer, 2019. High mountain areas. In: Pörtner, H.-O., Roberts, D.C., Masson-Delmotte, V., Zhai, P., Tignor, M., Poloczanska, E., Mintenbeck, K., Alegría, A., Nicolai, M., Okem, A., Petzold, J., Rama, B., Weyer, N.M. (Eds.), IPCC Special Report on the Ocean and Cryosphere in a Changing Climate In press.

Immerzeel, W.W., Lutz, A.F., Andrade, M., Bahl, A., Biemans, H., Bolch, T., Hyde, S., Brumby, S., Davies, B.J., Elmore, A.C., Emmer, A., 2020. Importance and vulnerability of the world's water towers. Nature 577 (7790), 364–369. https://doi.org/10.1038/s41586-019-1822-y.

Kääb, A., Berthier, E., Nuth, C., Gardelle, J., Arnaud, Y., 2012. Contrasting patterns of early twenty-first-century glacier mass change in the Himalayas. Nature 488, 495–498. https://doi.org/10.1038/nature11324.

Kääb, A., Treichler, D., Nuth, C., Berthier, E., 2015. Brief communication: contending estimates of 2003–2008 glacier mass balance over the Pamir-Karakoram-Himalaya. Cryosphere 9, 557–564. https://doi.org/10.5194/tc-9-557-2015.

Kamp, U., McManigal, K.G., Dashtseren, A., Walther, M., 2013. Glacial changes between 1910 and 2010 in the Turgen Mountains. Geogr. J. 179, 248–263. https://doi.org/10.1111/j.1475-4959.2012.00486.x.
Khan, A., Naz, B.S., Bowling, L.C., 2015. Separating snow, clean and debris covered ice in the Upper Indus Basin, Hindukush-Karakoram-Himalayas, using Landsat images between 1998 and 2002. J. Hydrol. 521, 46–64. https://doi.org/10.1016/j.jhydrol.2014.11.048.
Kick, W., 1967. Schlaginweits Vermessungsarbeiten am Nanga Parbat 1856. Deutsche Geodätische Kommission der Bayerischen Akademie der Wissenschaften 97. München.
Kick, W., 1994. Gletscherforschung am Nanga Parbat 1856–1990. Deutscher Alpenverein, München.
Kuhle, M., 1996. Rekonstruktion der maximalen eiszeitlichen Gletscherbedeckung im Nanga Parbat Massiv (35°05′-40°N/74°20′-75°E). In: Kick, W. (Ed.) Forschung am Nanga Parbat. Geschichte und Ergebnisse. Beiträge und Materialien zur Regionalen Geographie 8, 135–156 Berlin.
Kumar, V., Shukla, T., Mehta, M., Dobhal, D.P., Singh Bisht, M.P., Nautiyal, S., 2021. Glacier Changes and Associated Climate Drivers for the Last Three Decades, Nanda Devi Region, Central Himalaya, India. Quaternary International. doi:https://doi.org/10.1016/j.quaint.2020.06.017 (in press).
Lato, M.J., Frauenfelder, R., Bühler, Y., 2012. Automated detection of snow avalanche deposits: segmentation and classification of optical remote sensing imagery. Nat. Hazards Earth Syst. Sci. 12, 2893–2906. https://doi.org/10.5194/nhess-12-2893-2012.
Loewe, F., 1961. Glaciers of Nanga Parbat. Pakistan Geogr. Rev. 16, 19–24.
Mack, L., 2019. Surging Gletscher am Nanga Parbat? Eine Trendanalyse der Gletscherbewegungen mit optischen Satellitendaten. Unpublished Master Thesis. Heidelberg University.
Maurer, J.M., Rupper, S.B., Schaefer, J.M., 2016. Quantifying ice loss in the eastern Himalayas since 1974 using declassified spy satellite imagery. Cryosphere 10, 2203–2215. https://doi.org/10.5194/tc-10-2203-2016.
Muhammad, S., Tian, L., 2016. Changes in the ablation zones of glaciers in the western Himalaya and the Karakoram between 1972 and 2015. Remote Sens. Environ. 187, 505–512. https://doi.org/10.1016/j.rse.2016.10.034.
Muhammad, S., Tian, L., Nüsser, M., 2019a. No significant mass loss in the glaciers of Astore Basin (North-Western Himalaya), between 1999 and 2016. J. Glaciol. 65 (250), 270–278. https://doi.org/10.1017/jog.2019.5.
Muhammad, S., Tian, L., Khan, A., 2019b. Early twenty-first century glacier mass losses in the Indus Basin constrained by density assumptions. J. Hydrol. 574, 467–475. https://doi.org/10.1016/j.jhydrol.2019.04.057.
Muhammad, S., Tian, L., Ali, S., Latif, Y., Wazir, M.A., Goheer, M.A., Saifullah, M., Hussain, I., Shiyin, L., 2020. Thin debris layers do not enhance melting of the Karakoram glaciers. Sci. Total Environ. 746, 141119. https://doi.org/10.1016/j.scitotenv.2020.141119.
Mukul, M., Srivastava, V., Jade, S., Mukul, M., 2017. Uncertainties in the Shuttle Radar Topography Mission (SRTM) heights: insights from the Indian Himalaya and Peninsula. Sci. Rep. 7 (1), 41672. https://doi.org/10.1038/srep41672.
Neve, A., 1907. Rapid glacial advance in the Hindu Kush. Alp. J. 23, 400–401.
Nie, Y., Pritchard, H.D., Liu, Q., Hennig, T., Wang, W., Wang, X., Liu, S., Nepal, S., Samyn, D., Hewitt, K., Chen, X., 2021. Glacial change and hydrological implications in the Himalaya and Karakoram. Nat. Rev. Earth Environ. 2, 91–106. https://doi.org/10.1038/s43017-020-00124-w.
Nüsser, M., 2000. Change and persistence: contemporary landscape transformation in the Nanga Parbat area, northern Pakistan. Mt. Res. Dev. 20 (4), 348–355. https://doi.org/10.1659/0276-4741(2000)020[0348:CAPCLT]2.0.CO;2.
Nüsser, M., 2001. Understanding cultural landscape transformation: a re-photographic survey in Chitral, eastern Hindukush, Pakistan. Landsc. Urban Plan. 57 (3–4), 241–255. https://doi.org/10.1016/S0169-2046(01)00207-9.
Nüsser, M., 2015. Natur und Kultur im Himalaya: Die Gletscher- und Siedlungspanoramen der Brüder Schlagintweit. In: Brescius, M., Kaiser, F., Kleidt, S. (Eds.), Über den Himalaya. Die Expedition der Brüder Schlagintweit nach Indien und Zentralasien 1854–1858. Böhlau, Köln, pp. 319–343.
Nüsser, M., Baghel, R., 2014. The emergence of the cryoscape: Contested narratives of Himalayan glacier dynamics and climate change. Environmental and Climate Change in South and Southeast Asia: How Are Local Cultures Coping?Brill, Leiden, Boston, pp. 138–156 https://doi.org/10.1163/9789004273221_007.
Nüsser, M., Schmidt, S., 2017. Nanga Parbat revisited: evolution and dynamics of socio-hydrological interactions in the northwestern Himalaya. Ann. Am. Assoc. Geogr. 107 (2), 403–415. https://doi.org/10.1080/24694452.2016.1235495.
Paul, F., 2015. Revealing glacier flow and surge dynamics from animated satellite image sequences: examples from the Karakoram. Cryosphere 9, 2201–2214. https://doi.org/10.5194/tc-9-2201-2015.
Paul, F., 2019. A 60-year chronology of glacier surges in the central Karakoram from the analysis of satellite image time-series. Geomorphology 106993. https://doi.org/10.1016/J.GEOMORPH.2019.106993.
Paul, F., Huggel, C., Kääb, A., 2004. Combining satellite multispectral image data and a digital elevation model for mapping debris-covered glaciers. Remote Sens. Environ. 89, 510–518. https://doi.org/10.1016/j.rse.2003.11.007.
Paul, F., Barry, R.G., Cogley, J.G., Frey, H., Haeberli, W., Ohmura, A., Ommanney, C.S.L., Raup, B., Rivera, A., Zemp, M., 2010: Guidelines for the compilation of glacier inventory data from digital sources. Available at http://globglacier.ch/docs/guidelines_inventory.pdf (last accessed 19 February 2921).
Paul, F., Winsvold, S.H., Kääb, A., Nagler, T., Schwaizer, G., 2016. Glacier remote sensing using Sentinel-2. Part II: mapping glacier extents and surface facies, and comparison to Landsat 8. Remote Sens. 8 (7), 15. https://doi.org/10.3390/rs8070575.
Racoviteanu, A.E., Paul, F., Raup, B., Khalsa, S.J.S., Armstrong, R., 2009. Challenges and recommendations in mapping of glacier parameters from space: results of the 2008 Global Land Ice Measurements from Space (GLIMS) workshop, Boulder, Colorado, USA. Ann. Glaciol. 50(53) :53–69. doi:https://doi.org/10.3189/172756410790595804.
Rashid, I., Majeed, U., 2020. Retreat and geodetic mass changes of Zemu glacier, Sikkim Himalaya, India, between 1931 and 2018. Reg. Environ. Chang. 20, 125. https://doi.org/10.1007/s10113-020-01717-3.
Schlagintweit, H., 1872. Reisen in Indien und Hochasien. Band. vol. 3. Hermann Costenoble, Jena.
Schmidt, S., Nüsser, M., 2009. Fluctuations of Raikot Glacier during the last 70 years: a case study from the Nanga Parbat massif, northern Pakistan. J. Glaciol. 55 (194), 949–959. https://doi.org/10.3189/002214309790794878.
Schmidt, S., Nüsser, M., 2012. Changes of high altitude glaciers from 1969 to 2010 in the Trans-Himalayan Kang Yatze massif, Ladakh, Northwest India. Arct. Antarct. Alp. Res. 44 (1), 107–121. https://doi.org/10.1657/1938-4246-44.1.107.
Schmidt, S., Nüsser, M., 2017. Changes of high altitude glaciers in the Trans-Himalaya of Ladakh over the past five decades (1969–2016). Geosciences 7 (2), 27. https://doi.org/10.3390/geosciences7020027.
Shean, D., 2017. High Mountain Asia 8-meter DEM mosaics derived from optical imagery. Version. vol. 1. NASA National Snow and Ice Data Center Distributed Active Archive Center, Boulder, Colorado, USA. https://doi.org/10.5067/KXOVQ9L172S2.
Shroder, J.F., Bishop, M.P., Copland, L., Sloan. V.F., 2000. Debris-covered glaciers and rock glaciers in the Nanga Parbat Himalaya, Pakistan. Geografiska Annaler A 82 (1),17–31. doi:https://doi.org/10.1111/j.0435-3676.2000.00108.x.
Shukla, A., Ali, I., Hasan, N., Romshoo, S.A., 2017. Dimensional changes in the Kolahoi glacier from 1857 to 2014. Environ. Monit. Assess. 189, 5. https://doi.org/10.1007/s10661-016-5703-7.
Shukla, A., Garg, S., Mehta, M., Kumar, V., Shukla, U.K., 2020. Temporal inventory of glaciers in the Suru sub-basin, western Himalaya: impacts of regional climate variability. Earth Sys. Sci. Data 12, 1245–1265. https://doi.org/10.5194/essd-12-1245–2020.
Soheb, M., Ramanathan, A., Angchuk, T., Mandal, A., Kumar, N., Lotus, S., 2020. Mass-balance observation, reconstruction and sensitivity of Stok glacier, Ladakh region, India, between 1978 and 2019. J. Glaciol. 66 (258), 627–642. https://doi.org/10.1017/jog.2020.34.
Spohner, R., 2004. Rezente Landschaftsveränderungen im Nanga Parbat-Gebiet (Nordwest-Himalaya). PhD dissertation, Universität Bonn, Bonn.
Thakuri, S., Salerno, F., Smiraglia, C., Bolch, T., D'Agata, C., Viviano, G., Tartari, G., 2014. Tracing glacier changes since the 1960s on the south slope of Mt. Everest (central Southern Himalaya) using optical satellite imagery. Cryosphere 8, 1297–1315. https://doi.org/10.5194/tc-8-1297-2014.
Troll, C., 1938. Der Nanga Parbat als Ziel deutscher Forschung. Zeitschrift der Gesellschaft für Erdkunde zu Berlin 73, 1–26.
Winiger, M., Gumpert, M., Yamout, H., 2005. Karakorum-Hindukush-western Himalaya: assessing high-altitude water resources. Hydrol. Process. 19, 2329–2338. https://doi.org/10.1002/hyp.5887.
Wissmann, H. von, 1959. Die heutige Vergletscherung und Schneegrenze in Hochasien mit Hinweisen auf die Vergletscherung der letzten Eiszeit. Akademie der Wissenschaften und der Literatur in Mainz. Abhandlungen der Mathematisch-Naturwissenschaftlichen Klasse 14, 1103–1431.
Young, N.E., Anderson, R.S., Chignell, S.M., Vorster, A.G., Lawrence, R., Evangelista, P.H., 2017. A survival guide to Landsat preprocessing. Ecology 98, 920–932. https://doi.org/10.1002/ecy.1730.
Zhou, Y., Li, Z., Li, J., 2017. Slight glacier mass loss in the Karakoram region during the 1970s to 2000 revealed by KH-9 images and SRTM DEM. J. Glaciol. 63, 331–342. https://doi.org/10.1017/jog.2016.142.